Electron-hole pair production at metal surfaces

B. N. J. Persson and E. Zaremba*
Institut für Festkörperforschung, Kernforschungsanlage Jülich, D-5170 Jülich, West Germany
(Received 25 June 1984)

We discuss the response of a metal surface to an external electric field which varies slowly in space and time. An earlier calculation of the power absorption due to the creation of electron-hole pairs is improved with the inclusion of an interference term between "bulk" and "surface" excitation processes. With these improvements, we obtain excellent agreement with the measured inelastic-electron-scattering cross section for Cu(100).

I. INTRODUCTION

The response of a metal surface to an external electromagnetic wave enters many important problems in surface science.[1] Despite this, our present understanding of the dynamic behavior of realistic metal surfaces is far from complete.[1,2] Because of their complex electronic structure, a quantitative analysis of the response properties of transition-metal surfaces is still out of reach and for this reason most of the theoretical effort has focused on the simple metals. However, even in this latter case it is now known that a self-consistent treatment of the surface electronic structure is necessary in order to obtain a realistic description of the surface response properties. Calculations based on simple models, such as the infinite barrier or hydrodynamic models, have shown that such models are often too crude to provide a quantitative (and in some cases even qualitative) explanation of experimental data.

The most realistic calculations presented so far for the simple metals have been those by Feibelman,[1,3] Persson *et al.*[4] and Eguiluz.[5] All these calculations make use of a jellium model in which the metal ion cores are smeared out into a uniform positive background which terminates abruptly at the surface plane. The rationale for the model is that the ionic potentials are effectively weak and therefore do not influence significantly the characteristic response of the valence electrons. The ground-state electron density profile can be calculated self-consistently using a density functional theory as in the work of Lang and Kohn.[6] The surface potential and corresponding single-particle electronic states can then be used to treat the dynamic response within the random-phase approximation (RPA). With this approach, Feibelman has studied in considerable detail the nature of the charges and currents induced by an external electromagnetic field which varies slowly in space ($q_{||}/k_F \ll 1$) but rapidly in time ($\omega \gtrsim \omega_p/2$). The very good agreement achieved between these calculations and the surface photoelectric measurement of Levinson *et al.* for Al,[7] supports the validity of the jellium model in this case.

For optical radiation, the incident fields indeed have a slow variation along the surface of the metal and are characterized by a parallel wave vector $q_{||} \ll k_F$. Exploiting this small parameter, Feibelman was able to calculate the leading corrections in $q_{||}$ to the reflectivity factors for s- and p-polarized light which take into account the nonlocal dielectric response of the metal surface. It is important to note, however, that in a dynamic situation two independent parameters characterize the response of the metal, namely $q_{||}/k_F$ and $\eta^{-1} \equiv q_{||} v_F/\omega$. Expansions in powers of $q_{||}$ are possible only if *both* of these parameters are small compared to unity, a situation reached for arbitrary frequency when $q_{||}$ is sufficiently small. The parameter η^{-1} is a measure of the relative magnitude of the Fermi velocity to the phase velocity of a wavelike disturbance propagating along the surface. Its physical importance is related to the fact that an external field can excite electron-hole pairs more effectively for $\eta < 1$ than for $\eta > 1$. The sharp Fermi cutoff in the electron state occupation is ultimately the origin of the nonanalytic behavior found in various response functions at $\eta = 1$.

In contrast to the situation considered by Feibelman, the work of Persson and Lang and Persson and Andersson[4] is concerned with the low-frequency regime ($\omega \ll \omega_p$), where in general it is not possible to perform an expansion in $q_{||}$. The inelastic scattering of low-energy electrons from a metal surface is one example in which values of the parameter $q_{||} v_F/\omega$ greater than unity are encountered. The electric field of the incident electron penetrates into the metal where, in particularly, it can excite electron-hole pairs. In the so-called dipole-scattering regime, the momentum transfered to the excitation is small, being given by $q_{||} \sim k_0 \hbar\omega/2E_0$ (where $E_0 = \hbar^2 k_0^2/2m$ is the kinetic energy of the incident electron), so that in this case $q_{||} v_F/\omega \sim k_F/k_0 > 1$ if $E_0/\varepsilon_F < 1$. In Ref. 4 it was shown that with a few plausible assumptions it is possible to determine the dielectric response for arbitrary η provided $q_{||}/k_F$ and $\omega/\varepsilon_F \ll 1$. The resulting theory was found to be consistent with Andersson's data for inelastic-electron scattering from Cu(100). This theory, however, was incomplete and one aim of the present paper is to study in more detail some of the assumptions made by Persson and Andersson. In particular, the separation of the surface and bulk excitation of electron-hole pairs is examined more critically and their interference, previously neglected, will be calculated. This analysis leads to an improved and more consistent explanation of the experimental data.

Finally, we wish to comment on the possibility of extending our results beyond the small $q_{||}/k_F$ and small $\hbar\omega/\varepsilon_F$ limit. The approach of Eguiluz[5] is based on the

study of a jellium film geometry and in principle is valid for arbitrary $q_{||}$ and ω. However, if the thin slab is to represent semi-infinite jellium, then the film thickness must satisfy $L \gg 1/q_{||}$. Thus, from a practical point of view, it is difficult to study the small $q_{||}$ limit using this method. Nevertheless, it does provide a way to go beyond the small $q_{||}$ limit which is now quite well understood from the work discussed above and in the present paper.

The paper is organized as follow: In Sec. II we review some basic equations necessary for the following sections. In Sec. III we evaluate the interference term between bulk and surface excitation of electron-hole pairs and in Sec. IV the theoretical results are compared with experimental data. Section V contains our conclusions.

II. SOME BASIC CONCEPTS AND EQUATIONS

In this section, we will review some basic concepts and equations which are required in the following sections. Assume that a semi-infinite jellium occupies the half-space $z<0$ and consider the response of this system to an external electric potential of the form

$$\phi_{\rm ext}=e^{q_{||}z}e^{i(\mathbf{q}_{||}\cdot\mathbf{x}-\omega t)}+\text{c.c.} \tag{1}$$

An arbitrary electric potential can always be decomposed into evanscent plane waves of this type in a region of space where there are no external charges, $\nabla^2\phi_{\rm ext}=0$. The external potential (1) will give rise to an induced potential which outside the metal ($z>0$) can be written as

$$\phi_{\rm ind}=-g(q_{||},\omega)e^{-q_{||}z}e^{i(\mathbf{q}_{||}\cdot\mathbf{x}-\omega t)}+\text{c.c.} \tag{2}$$

This equation defines the linear-response function $g(q_{||},\omega)$. It has been implicitly assumed that the external potential $\phi_{\rm ext}$ is so weak that the metal responds linearly to it. The function $g(q_{||},\omega)$ is itself related to the density response function of the metal by

$$g(q_{||},\omega)=\frac{2\pi}{q_{||}}\int dz\int dz'\,e^{q_{||}z}e^{q_{||}z'}\chi(z,z',q_{||},\omega)$$
$$\equiv-\int dz\,e^{q_{||}z}\rho_{\rm ind}(z,q_{||},\omega)\ , \tag{3}$$

where the second equality defines the induced surface charge density.

The quantity Img can be identified with the power absorption in the metal due to the electronic excitations induced by the evanscent external potential (1). As such, it is given in terms of the total transition rate, w, by the useful relation

$$\text{Im}g=\pi\hbar w/(Aq_{||})\ , \tag{4}$$

where A is the surface area. This equation, which has been used in several earlier works, is proved in Appendix A.

In the standard textbook treatment of the dielectric response of a metal surface, one assumes that the solid is characterized by a local dielectric function $\epsilon(\omega)$ which jumps discontinuously at the surface, i.e., $\epsilon=\epsilon(\omega)$ for $z<0$ and $\epsilon=1$ for $z>0$. From the continuity of ϕ and $\epsilon\,d\phi/dz$ at the solid-vacuum interface, one obtains the well-known result

$$g(q_{||},\omega)=\frac{\epsilon(\omega)-1}{\epsilon(\omega)+1}\ , \tag{5}$$

which is independent of $q_{||}$ because of the assumed local dielectric response. A real metal does not have a steplike surface profile but a profile which varies smoothly on a microscopic scale. Furthermore, the dielectric properties of the surface are characterized by a nonlocal tensor, $\epsilon_{\mu\nu}(z,z',q_{||},\omega)$ which depends on z and z' as well as the wave vector $q_{||}$. Thus (5) is not correct for arbitrary $q_{||}$ although one can prove that it is exact for $q_{||}=0$.

Feibelman[1,3] has shown that the leading correction in $q_{||}$ to (5) can be written as (with the jellium positive background edge located at the origin)

$$g(q_{||},\omega)=\frac{\epsilon(\omega)-1}{\epsilon(\omega)+1}+2q_{||}d_\perp(\omega)\frac{\epsilon(\omega)[\epsilon(\omega)-1]}{[\epsilon(\omega)+1]^2}+O(q_{||}^2)\ . \tag{6}$$

This expansion in $q_{||}$ is useful if $q_{||}/k_F\ll 1$ *and* when the parameter $\eta^{-1}=q_{||}v_F/\omega\ll 1$. [Actually (6) also gives the correct zero-frequency result, $g(q_{||},0)=1+2q_{||}d_\perp(0)$. However, it cannot be inferred from this that (6) remains valid for arbitrary η. The fact that $g(q_{||},\omega)$ does not in general admit an expansion of this type is associated with its nonanalytic behavior at $\eta=1$. See Eq. (33).] The linear-response function $d_\perp(\omega)$ occurring in (6) is the centroid of the induced charge density, i.e.,

$$d_\perp(\omega)=\frac{\int_{-\infty}^{\infty}dz\,z\rho_{\rm ind}(z,\omega)}{\int_{-\infty}^{\infty}dz\,\rho_{\rm ind}(z,\omega)}\ . \tag{7}$$

For $\omega\neq 0$, $d_\perp(\omega)$ is a complex number. It defines the frequency-dependent image-plane position according to the formula

$$d_{\rm IP}(\omega)=\frac{\epsilon(\omega)}{\epsilon(\omega)+1}d_\perp(\omega)\ . \tag{8}$$

In the static limit ($\omega=0$), (8) reduces to $d_\perp(0)$ which is the reference plane position of the image potential for an external point charge. The absorptive part of the centroid, $\text{Im}d_\perp(\omega)$, represents the absorption due to the real excitation of electron-hole pairs and to plasmons, if $\omega>\omega_P$.

It is clear from (6) that $d_\perp(\omega)$ is a causal response function [because both $\epsilon(\omega)$ and $g(q_{||},\omega)$ are causal response functions] and that it therefore fulfills the Kramers-Kronig relations[8]

$$\text{Re}d_\perp(\omega)=\frac{2}{\pi}\text{P}\int_0^\infty d\omega'\frac{\omega'\text{Im}d_\perp(\omega')}{(\omega')^2-\omega^2}\ , \tag{9}$$

$$\text{Re}d_\perp(\omega)=-\frac{2}{\pi}\text{P}\int_0^\infty d\omega'\frac{\omega\text{Re}d_\perp(\omega')}{(\omega')^2-\omega^2}\ , \tag{10}$$

From these relations and the known high-frequency behavior of $d_\perp(\omega)$,[9] one can derive several useful sum rules, e.g.,

$$\int_0^\infty d\omega\,\omega\text{Im}d_\perp(\omega)=\eta(r_s)\omega_P^2\ , \tag{11}$$

$$\int_0^\infty d\omega\,\text{Re}d_\perp(\omega)=0\ , \tag{12}$$

where[9]

$$\eta(r_s)=\frac{\pi}{2}\int_0^\infty dz\, n_0(z) \tag{13}$$

only depends on the ground-state electron density profile, $n_0(z)$, normalized so that $n_0(z)\to 1$ as $z\to-\infty$. The parameter $\eta(r_s)$ determines the behavior of $d_\perp(\omega)$ for large ω via

$$d_\perp(\omega)\sim-\frac{2}{\pi}\eta\left[\frac{\omega_P}{\omega}\right]^2 . \tag{14}$$

Furthermore, we observe that the integrand in Eq. (12) must change sign so that as a function of frequency, the real part of the centroid will pass from one side of the jellium background edge to the other. We finally note that if $\mathrm{Im}d_\perp(\omega)$ has the low-frequency behavior,

$$\mathrm{Im}d_\perp(\omega)=\frac{\bar{\xi}}{k_F}\frac{\omega}{\omega_P},\quad \omega\ll\omega_P \tag{15}$$

as is found to be the case, then the following relation is fulfilled:

$$\frac{\bar{\xi}}{k_F\omega_P}=-\mathrm{P}\int_{-\infty}^{\infty}\frac{d\omega}{\pi}\frac{\mathrm{Re}d_\perp(\omega)}{\omega^2} , \tag{16}$$

The parameter $\bar{\xi}$ is determined in the following section.

III. EXCITATION OF ELECTRON-HOLE PAIRS FOR SMALL $q_\parallel$ AND ω

In this section we will study the structure of $\mathrm{Im}g(q_\parallel,\omega)$ for small $q_\parallel$ and ω. This problem has been considered in an earlier paper[4] where, however, a contribution to Img coming from the interference between the "bulk" and "surface" excitation of electron-hole pairs was neglected. We will calculate this term here and discuss under what conditions it is important. An alternative derivation of Img is given in Appendix B.

Following Ref. 4, Img is calculated from (4) as follows. First, we calculate the rate at which the external potential (3) excites electron-hole pairs in the metal. Using the golden rule formula, we get (a.u.)

$$w=2\pi\int d^3k\, d^3k'(f_k-f_{k'}) \times|\langle k'|\phi|k\rangle|^2\delta(\varepsilon_{k'}-\varepsilon_k-\omega) , \tag{17}$$

in which matrix elements of the complex total potential, $\phi=\phi_{\mathrm{ext}}+\phi_{\mathrm{ind}}$, appear (see Appendix B). Here f_k is the finite-temperature Fermi-Dirac distribution function.

Secondly, we require an expression for the total potential

$$\phi(z,q_\parallel,\omega)=e^{q_\parallel z}+\int dz'\, e^{-q_\parallel|z-z'|}\rho_{\mathrm{ind}}(z',q_\parallel,\omega) , \tag{18}$$

which in general requires a self-consistent calculation of the induced charge density. However, we shall make use of the fact that for small $q_\parallel$ and ω, the integrated screening charge must be close to the classical electrostatic result. The modification of the real part of ρ_{ind} at low frequencies by electron-hole pair production is a weak effect and can be neglected when estimating ϕ to be used in (17). A similar approximation for $\mathrm{Im}\rho_{\mathrm{ind}}$ in (3) would of course be meaningless since Img depends explicitly on these excitation processes.

We assume that the surface screening charge is essentially localized within a microscopic width, a, of the surface. The total potential deep in the metal then behaves as

$$\phi(z,q_\parallel,\omega)\to e^{q_\parallel z}[1-Q(q_\parallel,\omega)] , \tag{19}$$

where

$$Q(q_\parallel,\omega)=-\int dz\, e^{-q_\parallel z}\rho_{\mathrm{ind}}(z,q_\parallel,\omega) . \tag{20}$$

The quantity $Q(q_\parallel,\omega)$ is closely related to $g(q_\parallel,\omega)$, differing only in the sign of the exponent in (20). It can be expanded in a similar fashion to $g(q_\parallel,\omega)$ in (6),

$$Q(q_\parallel,\omega)=\frac{\epsilon(\omega)-1}{\epsilon(\omega)+1}-2q_\parallel d_\perp(\omega)\frac{\epsilon(\omega)-1}{[\epsilon(\omega)+1]^2}+O(q_\parallel^2) . \tag{21}$$

This result is strictly valid in the large η limit. That the coefficient of $q_\parallel$ vanishes when $\omega=0$ is, however, an exact result and suggests that the second term in (21) can be neglected when considering the real part of $Q(q_\parallel,\omega)$ in the long-wavelength limit. This quantity then depends only on the frequency through the bulk dielectric function. Writing $\epsilon(\omega)=1-(\omega_P^2/\omega^2)(m/m_{\mathrm{opt}})$ for the low-frequency behavior, where $\omega_p^2=4\pi ne^2/m$ is the jellium plasma frequency and m_{opt} is the optical mass, (21) reduces to (neglecting the second term)

$$Q(q_\parallel,\omega)=1+\frac{m_{\mathrm{opt}}}{m}\frac{2\omega^2}{\omega_P^2}+\cdots . \tag{22}$$

In the jellium model, m_{opt} is, of course, the free-electron mass but we have allowed for a more general situation with the application to Cu in mind.

We now *define* the *bulk* potential ϕ_{bulk} to be of the form (19) throughout *all* space and the surface potential by the difference

$$\phi_{\mathrm{surf}}(z,q_\parallel,\omega)=\phi(z,q_\parallel,\omega)-\phi_{\mathrm{bulk}}(z,q_\parallel,\omega) . \tag{23}$$

The surface part can be shown to satisfy the equation

$$\frac{d^2\phi_{\mathrm{surf}}}{dz^2}=-2q_\parallel\rho_{\mathrm{ind}}(z,q_\parallel,\omega) +q_\parallel^2\int dz'(e^{-q_\parallel|z-z'|}-e^{q_\parallel(z-z')})\rho_{\mathrm{ind}}(z',q_\parallel,\omega) . \tag{24}$$

The second term on the right-hand side vanishes in the interior of the metal and is of order $q_\parallel a$ relative to the first in the surface region. Thus, it can be neglected in the evaluation of ϕ_{surf}. Furthermore, for the small values of $q_\parallel$ and ω of interest, we can replace $\rho_{\mathrm{ind}}(z,q_\parallel,\omega)$ by $\rho_{\mathrm{ind}}^0(z)\equiv\rho_{\mathrm{ind}}(z,0,0)$ which is the charge density induced by a static uniform electric field perpendicular to the surface. This quantity has been calculated by Lang and Kohn. Its use in (24) leads to the surface potential considered by Persson and Lang, $\phi_{\mathrm{surf}}=-(q_\parallel/2\pi)A(z)$ with $A(z)$ the solution of

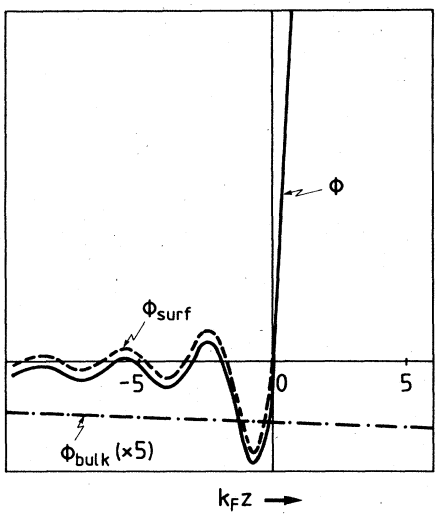

FIG. 1. Electric potential ϕ (equal to external plus induced potential) in the surface region of a metal due to an external current distribution. Relative magnitudes of the surface and bulk contributions ($\phi=\phi_{\rm surf}+\phi_{\rm bulk}$) are representative of $r_s=3$ jellium for $\hbar\omega\sim 0.1$ eV and $q_{||}\sim 0.02$ Å^{-1}.

$$\frac{d^2A(z)}{dz^2}=4\pi\rho^0_{\rm ind}(z)\ . \tag{25}$$

$A(z)$ is the induced potential in the metal due to a uniform charged sheet outside the metal surface and carrying one unit of charge per unit area. Apart from Friedel oscillations, $\phi_{\rm surf}$ is localized in the surface region.

Finally the bulk potential from (19) and (22) is given by

$$\phi_{\rm bulk}(z)=-\frac{m_{\rm opt}}{m}\frac{2\omega^2}{\omega_P^2}e^{q_{||}z}\ . \tag{26}$$

We note that the amplitude of $\phi_{\rm bulk}$ is negative relative to the external potential implying that the surface charge density overscreens the externally applied field at finite frequencies. The total potential and its decomposition into bulk and surface terms is shown schematically in Fig. 1. Equations (25) and (26) are expected to provide an accurate representation of ϕ in the small $q_{||}$ and ω limit.

We thus have

$$\langle k'\,|\,\phi\,|\,k\rangle=\langle k'\,|\,\phi_{\rm surf}\,|\,k\rangle+\langle k'\,|\,\phi_{\rm bulk}\,|\,k\rangle$$

and the rate w will have three contributions,

$$w=w_{\rm surf}+w_{\rm bulk}+w_{\rm int}\ .$$

The interference term $w_{\rm int}$ was neglected in the treatment presented in Ref. 4 but we will consider it here. It was shown in Ref. 4 that

$$\langle k'\,|\,\phi_{\rm surf}\,|\,k\rangle=-\frac{q_{||}}{\pi^2}\delta(\mathbf{k}_{||}+\mathbf{q}_{||}-\mathbf{k}'_{||})\langle\psi_{k'_z}\,|\,A\,|\,\psi_{k_z}\rangle$$

and

$$\langle k'\,|\,\phi_{\rm bulk}\,|\,k\rangle=-\frac{2}{\pi}\left[\frac{m_{\rm opt}}{m}\right]\left[\frac{\omega}{\omega_P}\right]^2\times\delta(\mathbf{k}_{||}+\mathbf{q}_{||}-\mathbf{k}'_{||})\frac{q_{||}}{q_{||}^2+(k_z-k'_z)^2}\ .$$

We write

$$\langle k'\,|\,(\phi_{\rm surf}+\phi_{\rm bulk})\,|\,k\rangle=-\frac{q_{||}}{\pi^2k_F^2}\delta(\mathbf{k}_{||}+\mathbf{q}_{||}-\mathbf{k}'_{||})M_{kk'} \tag{27}$$

so that

$$M_{kk'}=\langle\psi_{k'_z}\,|\,Ak_F^2\,|\,\psi_{k_z}\rangle+2\pi\left[\frac{m_{\rm opt}}{m}\right]\left[\frac{\omega}{\omega_P}\right]^2\frac{k_F^2}{q_{||}^2+(k_z-k'_z)^2}\ . \tag{28}$$

Using (17) and (27) and accounting for the electron spin [which introduces an extra factor of 2 in (17)] we get

$$w=4\pi\frac{A}{(2\pi)^2}\left[\frac{q_{||}}{\pi^2k_F^2}\right]^2\int d^3k(f_\varepsilon-f_{\varepsilon'})\,|\,M_{kk'}\,|^2/k'_z\ , \tag{29}$$

where $\mathbf{k}'_{||}=\mathbf{k}_{||}+\mathbf{q}_{||}$ and $\varepsilon'=\varepsilon+\omega$. In deriving (29) we have used the identity

$$|\,\delta(\mathbf{k}_{||})\,|^2=\frac{A}{(2\pi)^2}\delta(\mathbf{k}_{||})\ ,$$

where A is the surface area. Substituting (29) into (4) gives

$$\mathrm{Im}g=\frac{q_{||}}{\pi^4k_F^4}\int d^3k(f_\varepsilon-f_{\varepsilon'})\,|\,M_{kk'}\,|^2/k'_z\ . \tag{30}$$

Now, if $F(\mathbf{k})$ is an arbitrary function of $\mathbf{k}$ which varies slowly with ε, then we have for $\omega\ll\varepsilon_F$,

$$\begin{aligned}&\int d^3k(f_\varepsilon-f_{\varepsilon+\omega})F(\mathbf{k})\\&=\int d\varepsilon\,k(f_\varepsilon-f_{\varepsilon+\omega})\int d\Omega_{\mathbf{k}}F(\mathbf{k})\\&\approx\omega k_F\int d\Omega_{\mathbf{k}}F(\mathbf{k})\,|_{\,k=k_F}\\&\approx\omega\int_0^{2\pi}d\varphi\int_0^{k_F}dk_z\,F(\mathbf{k})\,|_{\,k=k_F}\ .\end{aligned} \tag{31}$$

This is precisely the result one would have obtained in the zero-temperature limit. From (30) and (31) we get

$$\mathrm{Im}g=\frac{q_{||}\omega}{\pi^4k_F^4}\int_0^{k_F}dk_z\frac{1}{k_z}\int_0^{2\pi}d\varphi\,|\,M_{kk'}\,|^2\ . \tag{32}$$

Substituting (28) in (32) we obtain the following after some simplications:

$$\mathrm{Im}g=(\mathrm{Im}g)_{\rm surf}+(\mathrm{Im}g)_{\rm bulk}+(\mathrm{Im}g)_{\rm int}\ ,$$

where

$$\begin{aligned}(\mathrm{Im}g)_{\rm surf}&=2\xi\frac{q_{||}}{k_F}\frac{\omega}{\omega_P}\ ,\\(\mathrm{Im}g)_{\rm bulk}&=\frac{1}{2}\left[\frac{m_{\rm opt}}{m}\right]^2\left[\frac{\omega}{\omega_P}\right]^2\eta^3G(\eta)\ ,\\(\mathrm{Im}g)_{\rm int}&=-\frac{8}{\pi^2}\frac{m_{\rm opt}}{m}\frac{1}{k_Fa_0}\left[\frac{\omega}{\omega_P}\right]^2\eta H(\eta)\ ,\end{aligned} \tag{33}$$

with

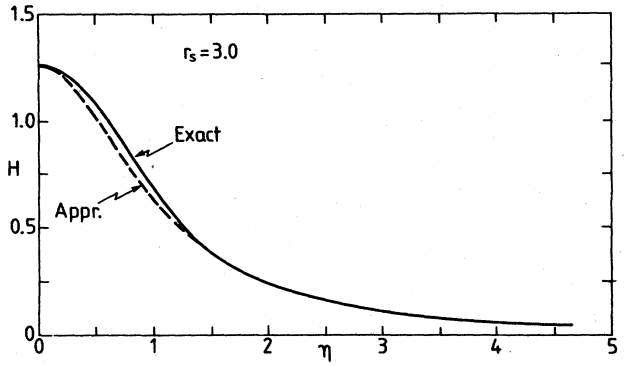

FIG. 2. Function $H(\eta)$ as given by Eq. (35). The curve denoted by "Appr." is the approximation given by Eq. (36).

$$G(\eta)=\begin{cases}8 & \text{for } \eta<1\\ 8[1-(1+\frac{1}{2}\eta^{-2})(1-\eta^{-2})^{1/2}] & \text{for } \eta>1\end{cases} \tag{34}$$

and

$$H(\eta)=\mathrm{Im}\left[\int_0^{k_F} dk_z \frac{1}{k_F}\frac{\langle\psi_{k_z}\mid Ak_F^2\mid\psi_{k_z}\rangle}{(\eta^2-1-2i\eta k_z/k_F)^{1/2}}\right]. \tag{35}$$

The third equation in (33) is the new interference term not included previously. We also note in passing that the second term in (33) differs from that used in Ref. 4 by the factors of the optical mass and a factor of $\frac{1}{2}$ which was missed previously.

Since the matrix element $\langle\psi_{k_z}\mid Ak_F^2\mid\psi_{k_z}\rangle$ is strongly peaked for $k_z=k_F$ (see Ref. 4) we have as a good approximation

$$\begin{aligned}H(\eta)&\approx\mathrm{Im}\left[\frac{1}{(\eta^2-1-2i\eta)^{1/2}}\times\int_0^{k_F}dk_z\frac{1}{k_F}\langle\psi_{k_z}\mid Ak_F^2\mid\psi_{k_z}\rangle\right]\\&=\frac{h(r_s)}{1+\eta^2},\end{aligned} \tag{36}$$

where

$$h(r_s)=\int_0^{k_F}dk_z\frac{1}{k_F}\langle\psi_{k_z}\mid Ak_F^2\mid\psi_{k_z}\rangle. \tag{37}$$

In Fig. 2 we compare (for $r_s=3$) the exact expression for $H(\eta)$ with the approximate formula (36). The function $h(r_s)$ is given for $r_s=2$, 3, and 4 in Table I together with some other useful parameters introduced in Sec. II. All of the quantities in Table I are ground-state quantities which have been calculated using the local-density approximation of the density functional scheme.

From (33) we can obtain an expression for $d_\perp(\omega)$ valid for $\omega\ll\omega_P$. First note that for $\omega\ll\omega_P$, (6) reduces to

$$g(q_{||},\omega)=1+2q_{||}d_\perp(\omega)+O(q_{||}^2)$$

or

$$\mathrm{Im}\,g(q_{||},\omega)=2q_{||}\mathrm{Im}\,d_\perp(\omega)+O(q_{||}^2). \tag{38}$$

For $q_{||}\to 0$ and ω fixed, $\eta\to\infty$ and we have

$$H(\eta)\sim\frac{1}{\eta^2}\int_0^{k_F}dk_z\frac{1}{k_F}\frac{k_z}{k_F}\langle\psi_{k_z}\mid Ak_F^2\mid\psi_{k_z}\rangle\equiv\frac{u}{\eta^2}$$

and $G(\eta)\sim 3/\eta^4$. Substituting this in (33) gives

$$\mathrm{Im}\,g=2\bar{\xi}\frac{q_{||}}{k_F}\frac{\omega}{\omega_P}, \tag{39}$$

where

$$\bar{\xi}=\xi+\frac{3}{2}\left[\frac{m_{\mathrm{opt}}}{m}\right]^2\frac{\omega_F}{\omega_P}-\frac{8}{\pi^2}\frac{m_{\mathrm{opt}}}{m}\frac{u}{k_Fa_0}\frac{\omega_F}{\omega_P}. \tag{40}$$

Explicit expressions for ξ and $\bar{\xi}$ are given in Appendix B. Comparing (38) and (39) we see that $\mathrm{Im}\,d_\perp(\omega)\sim\omega$ as $\omega\to 0$ as previously claimed. In Table I we give $\bar{\xi}$ for $r_s=2$, 3, and 4.

These results for $\bar{\xi}$ define the low-frequency behavior of $\mathrm{Im}\,d_\perp(\omega)$ which can be compared with the numerical calculations of Feibelman.[1] Although the two sets of calculations do not overlap in frequency, the extrapolation of the low-frequency behavior as defined in Eq. (40) is consistent with the numerical results obtained at higher frequencies. This comparison is discussed in more detail in Ref. 9 in the context of the van der Waals interaction of an atom with a metal surface. There it is shown that the use of the $\bar{\xi}$ values as given by Eq. (40) leads to an approximate satisfaction of the exact sum rule given by Eqs. (11) and (13). Thus, there is independent evidence to suggest that Eq. (33) indeed gives a reliable description of the low-frequency, long-wavelength absorptive response of free-electron-like metal surfaces.

TABLE I. The values of ξ [defined in (B15)] are taken from Ref. 8. $\bar{\xi}$ and h are evaluated using Eqs. (40) and (37), respectively. $\eta(r_s)$ as given by (13) is calculated using the equilibrium jellium density profile of Ref. 6. The static centroid $d_\perp(0)$ is taken from Ref. 17.

r_s	ξ	$\bar{\xi}$	$\eta(r_s)$	$d_\perp(0)/a_0$	h
2	2.359	1.041	0.72	1.60	4.29
3	0.296	0.368	0.85	1.42	1.26
4	0.0939	0.482	0.94	1.30	0.496
2.67 (Cu, interpolation)	0.49	0.460	0.82	1.47	1.84

IV. COMPARISON OF THEORY WITH EXPERIMENTAL DATA

It has recently been shown that $\mathrm{Img}(q_{||},\omega)$ can be measured directly using inelastic electron scattering from clean metal surfaces. Such measurements have been performed by Andersson *et al.*[10] on Cu(100), and here, we will compare his experimental data with the theory for Img presented in the last section. We will start with a brief review of electron-energy-loss spectroscopy (EELS).

Consider an electron with a few eV energy incident upon the surface. The electric field from the electron penetrates into the medium where it can excite, e.g., electron-hole pairs, plasmons, or phonons. Let $\mathbf{k}$ and $\mathbf{k}'$ denote the wave vectors of an incident and inelastically scattering electron, respectively. Thus, $\hbar\mathbf{q}_{||}=\hbar(\mathbf{k}_{||}-\mathbf{k}'_{||})$ is the momentum transfer (parallel to the surface) to the excitation, in the medium and $\hbar\omega=\hbar^2(k^2-k'^2)/2m$ is the energy transfer. Let $P(\mathbf{k},\mathbf{k}')d\Omega_{\mathbf{k}'}d(\hbar\omega)$ be the probability that an incident electron is scattered inelastically into the range of energy losses between $\hbar\omega$ and $\hbar(\omega+d\omega)$ and into the solid angle $d\Omega_{k'}$ around the direction of $\mathbf{k}'$. For small momentum transfer, $q_{||}\ll k$, one has from standard dipole-scattering theory[11]

$$P(\mathbf{k},\mathbf{k}')=\frac{2}{(ea_0\pi)^2}\frac{1}{\cos\alpha}\frac{k'}{k}\frac{q_{||}}{|q_{||}^2+q_\perp|^2}(n_\omega+1)\mathrm{Img}(q_{||},\omega)$$

$$\equiv A(\mathbf{k},\mathbf{k}')\mathrm{Img}(q_{||},\omega)\ , \tag{41}$$

where $q_\perp=k_z-k'_z$ and where α is the angle of incidence and n_ω the Bose-Einstein factor. Thus, the inelastic scattering probability is a product of two factors—a kinematic factor $A(\mathbf{k},\mathbf{k}')$ which depends strongly on the loss energy ($A\sim\omega^{-3}$ as $\omega\to 0$) but which is independent of the properties of the medium, and the loss function $\mathrm{Img}(q_{||},\omega)$ which is proportional to the power absorption in the medium due to an external potential of the form (1). $g(q_{||},\omega)$ enters the inelastic scattering probability (41) because it determines the induced electric field outside the substrate [via (2)] and it is this time varying field that can scatter the incident electron inelastically. Note that to obtain the scattering probability on the gain side ($\omega<0$) one must replace $(n_\omega+1)$ by $n_{|\omega|}$ in (41).

In the analysis presented below, we have actually used an improved dipole-scattering theory which accounts for the force on the incident electron from its own image in the metal surface. This scattering probability expression is somewhat more complicated than (41) and we refer the reader to Ref. 12 for the explicit expression.

The excitation process, which leads to the inelastic scattering probability (41), starts already when the incident electron is at large distance d from the surface where $d\sim(2E_0/\hbar\omega)/k_0$ with $E_0=\hbar^2k_0^2/2m$ being the kinetic energy of the incident electron. The momentum transfer is therefore small, $q_{||}\sim 1/d\sim k_0(\hbar\omega/2E_0)$ and the dipole-scattered electrons form a narrow lobe centered close to the specular direction. The width of the lobe is $\Delta\theta\sim\hbar\omega/2E_0$. In the experimental data to be discussed below, $E_0\sim 2$ eV, $\hbar\omega\sim 0.1$ eV so that $d\sim 40$ Å, $q_{||}\sim 0.02$ Å^{-1}, and $\Delta\theta\sim 1°$.

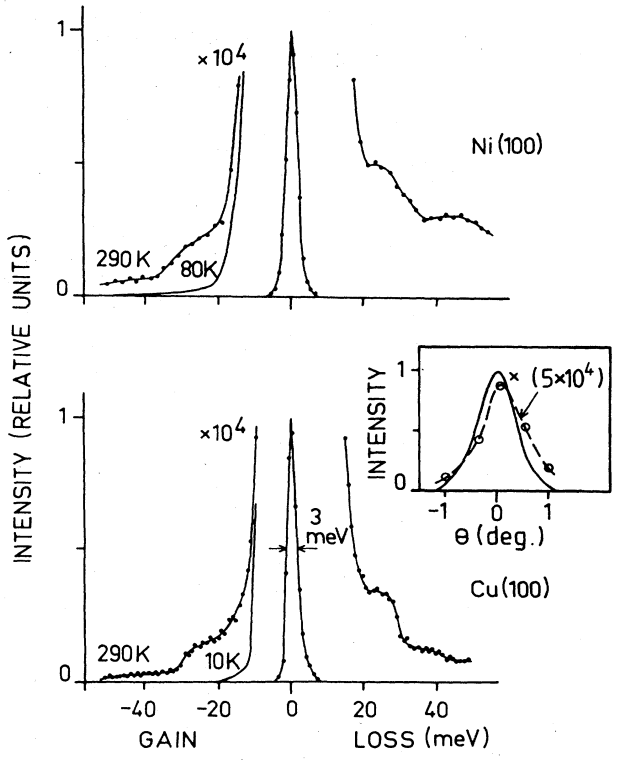

FIG. 3. Electron-energy-gain and -loss spectra from the Cu(100) and Ni(100) surfaces measured in the specular direction, $\theta=0°$, for a 2.3-eV electron-beam incident at 55°. The inset shows the elastic peak intensity (solid curve) and the inelastic intensity at 25 meV (open circles) for Cu(100) vs collection angle θ (positive towards the surface normal).

Equation (41) indicates that retardation effects always can be neglected in EELS involving slow electrons. This is formally proved by noting that the energy loss $\hbar\omega$ in dipole scattering is related to the momentum transfer $\hbar q_{||}$ via $q_{||}\sim(\hbar\omega/2E)k=\omega/v$ where v is the velocity of the incident electron. Thus, $q_{||}\gg\omega/c$ as long as $v\ll c$ (which, of course, is satisfied in EELS involving low-energy electrons) and retardation effects can therefore be neglected.

In EELS one does not measure $P(\mathbf{k},\mathbf{k}')$ directly, but rather $P(\mathbf{k},\mathbf{k}')$ integrated over the solid angle of detection

$$\Delta P(\omega)=\int_{\Delta\Omega}d\Omega_{\mathbf{k}'}P(\mathbf{k},\mathbf{k}')\ .$$

The experimental data discussed below were obtained with the analyzer in the specular direction (angle of incidence $\alpha=54°$) and with an acceptance angle (full width at half maximum) of 0.9°. Figure 3 shows electron-energy-loss data from Cu(100) and Ni(100) at room temperature and at a lower temperature.[13] The inelastic intensity on the loss side is proportional to $n_\omega+1$ while the intensity on the gain side is proportional to n_ω and thus smaller. For $|\omega|>\omega_0$, where ω_0 is the highest phonon frequency in the metal, it is only possible to excite electron-hole pairs while for $|\omega|<\omega_0$ phonons also can be excited. This explains the rather sharp change in the loss intensity at $\hbar\omega_0(\mathrm{Ni})\approx 36$ meV and $\hbar\omega_0(\mathrm{Cu})\approx 30$ meV which are the

highest longitudinal phonon frequencies in Ni and Cu, respectively, in the [100] direction. In what follows, we will only focus on the electron-hole pair continuum and refer the reader to Ref. 13 for a discussion of the phonon excitation process.

The energy-loss data analyzed below involves excitation of very low energetic electron-hole pairs, $\hbar\omega \sim 0.1$ eV. Thus, $\omega \ll \omega_P$ and $q_{\parallel} \ll k_F$ and we can use the expression for Img derived in Sec. III which we now write

$$\mathrm{Im}g = (\mathrm{Img})_{\mathrm{Drude}} + (\mathrm{Img})_{\mathrm{surf}} + (\mathrm{Img})_{\mathrm{bulk}} + (\mathrm{Img})_{\mathrm{int}} \ . \tag{42}$$

Here, we have added the Drude contribution

$$(\mathrm{Img})_{\mathrm{Drude}} = \mathrm{Im}\left[\frac{\epsilon(\omega)-1}{\epsilon(\omega)+1}\right] = 4\frac{\omega_F}{\omega_P}\frac{m_{\mathrm{opt}}}{m}\frac{1}{k_F l}\frac{\omega}{\omega_P} \tag{43}$$

representing phonon scattering in the bulk; $l = v_F \tau$ is the corresponding phonon mean free path. Note that $l \to \infty$ as $T \to 0$ so that the Drude contribution to Img vanishes as $T \to 0$. The other three terms in (42) are given explicitly in (33). For Cu we have $m_{\mathrm{opt}} \simeq 1.5$, and (see Table I) $\xi = 0.49$ and $h = 1.84$ so that

$$\mathrm{Im}g \approx \left[\frac{a}{k_F l} + b\frac{q_{\parallel}}{k_F} + c\eta^3 G(\eta)\frac{\omega}{\omega_P} + \frac{d\eta}{1+\eta^2}\frac{\omega}{\omega_P}\right]\frac{\omega}{\omega_P} \ ,$$

where $a = 3.89$, $b = 0.98$, $c = 1.125$, and $d = 3.10$.

Figure 4 shows how the inelastic scattering probability ΔP, for Cu(110), depends on the loss energy $\hbar\omega$. The inset shows the measured data[10] for ΔP at $\hbar\omega = 0.1$, 0.15, 0.2, and 0.3 eV and for several temperatures. We note that ΔP varies linearly with temperature which is also expected from optical data for copper. This is also the prediction

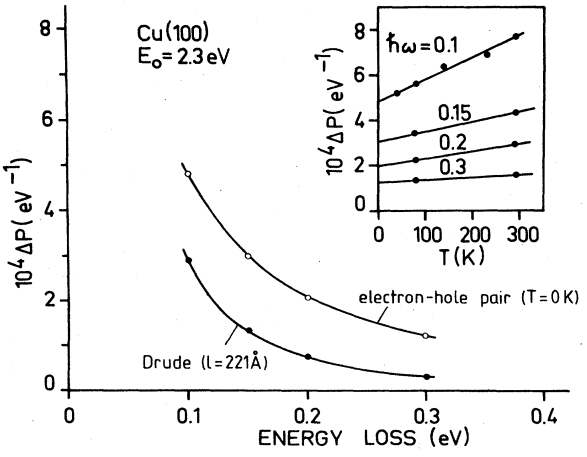

FIG. 4. Inelastic scattering probability ΔP vs loss energy, $\hbar\omega$, and temperature, T (see inset), for 2.3-eV electrons; specular condition. The open and solid circles represent the extrapolated experimental $\Delta P(T=0\ \mathrm{K})$ and $\Delta P(T=293\ \mathrm{K}) - \Delta P(T=0\ \mathrm{K})$ data, respectively. The solid curves are the theoretically predicted results for the Drude and electron-hole pair ($T=0$ K) contributions. The theoretically predicted electron-hole pair contribution has been scaled by a factor of 0.9 in order to emphasize the agreement with regard to the energy-loss dependence.

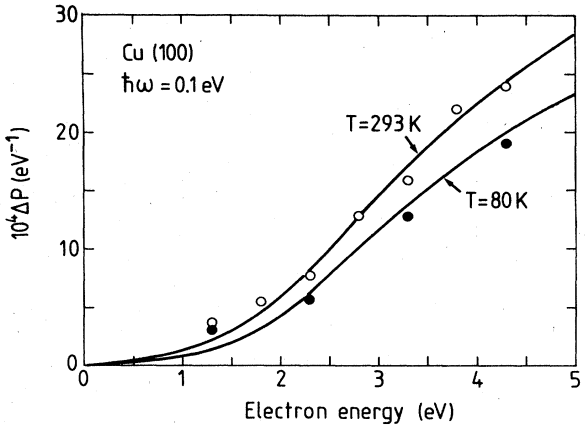

FIG. 5. Inelastic scattering probability ΔP vs incident electron energy. The open and solid circles denote the experimental ΔP values at $T=293$ K and $T=80$ K, respectively, for 0.1-eV loss energy and specular condition. The solid curves are the calculated results at the corresponding temperature.

from standard theory of phonon resistivity for $T > 0.2T_D$ (where T_D is the Debye temperature). The open circles in Fig. 4 correspond to the ΔP values obtained by extrapolating the data in the inset to $T=0$ K. The solid circles show the Drude contribution to ΔP at room temperature as given by $\Delta P(T=293\ \mathrm{K}) - \Delta P(T=0\ \mathrm{K})$. The solid curves are theoretically predicted results for ΔP using $\mathrm{Img} = (\mathrm{Img})_{\mathrm{surf}} + (\mathrm{Img})_{\mathrm{bulk}} + (\mathrm{Img})_{\mathrm{int}}$ for the upper curve and $\mathrm{Img} = (\mathrm{Img})_{\mathrm{Drude}}$ with $l = 221$ Å for the lower curve. We note that there is almost perfect agreement between theory and experiment with respect to the dependence of ΔP on the loss energy $\hbar\omega$. The absolute value ΔP in Fig. 4 deviates only by 10% from the theoretical result. Over a range of impact energies, the discrepancy on average is even less than this, as can be seen in Fig. 5. The open and solid circles correspond to experimental data for $\hbar\omega = 0.1$ eV obtained at 293 and 80 K substrate temperatures, respectively. The solid curves correspond to the calculated contribution using the expression for Img given by (42) for $T=293$ K ($l=221$ Å) and $T=0$ K ($l=0$ Å). The

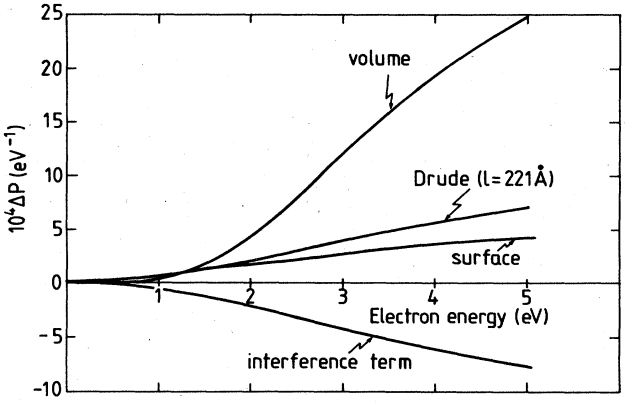

FIG. 6. Various components of the inelastic scattering probability as obtained from Eq. (42) contributing to the total result in Fig. 5.

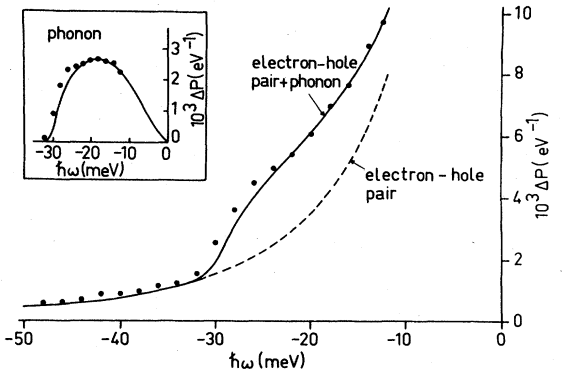

FIG. 7. Filled circles show the experimental gain probability, ΔP, for Cu(100) at 290 K. The dashed and solid curves show the calculated contributions to ΔP from electron-hole pair excitations and the sum of electron-hole pair and phonon excitations, respectively. The inset shows separately the experimental (solid curves) and calculate (solid curve) phonon contribution to ΔP. The theoretical electron-hole pair contribution is scaled with a factor of 1.2

agreement between theory and experiment is very good, with regard to the dependence of ΔP on the incident electron energy, the absolute value of ΔP and the relative magnitude of the Drude contribution. Figure 6 shows separately the various contributions to ΔP for the case shown in Fig. 5.

Figure 7 shows the function $\Delta P(\omega)$ on the gain side of the electron-energy-loss spectrum. The black dots are the experimental data points (the same as in Fig. 3) and the dashed line is the calculated contribution to ΔP using (41) but with $n_\omega+1$ replaced with $n_{|\omega|}$. The full line is the result obtained by adding a contribution caused by excitation of longitudinal bulk phonons, propagating normal to the metal surface into the bulk, as is described elsewhere.[13] Using the same parameters as above ($m_{\rm opt}=1.5$ m and $l=221$ Å) the contribution from excitation of electron-hole pairs deviates only by about 20% from the measured data points.

V. SUMMARY AND CONCLUSIONS

In this paper we have studied the excitation of electron-hole pairs at a metal surface by an external perturbation varying slowly in space and time. We have shown that the total self-consistent potential can be separated into bulk and surface parts which each contribute to the pair production rate. In an earlier treatment the interference between bulk and surface excitation processes had been neglected, but we find that it in general gives an important contribution to the loss function Img. Reanalyzing the experimental electron-energy-loss data of Andersson, we now find even better agreement between theory and experiment, with typical discrepancies being of the order of 10%. We note that the only adjusted parameter in the theory is the mean free path l.

However, there still remain a few questions which should be considered in more detail. Our results are based on the jellium approximation which obviously is not valid in the case of transition metals such as Ni. For the noble metals, the approximation is more reasonable since the low-frequency excitations are associated with a free-electron-like s-p band. One aspect of the electronic band structure has been included through the use of the appropriate bulk dielectric function in the definition of the bulk potential in Eq. (26). This leads to the appearance of the optical mass in Eq. (33). However, the nature of the electronic states will also influence the magnitude of the matrix element in Eq. (27). Since $\phi_{\rm bulk}$ is a slowly varying function of space, the replacement of plane-wave states by Bloch states will not affect this matrix element significantly. However, it is difficult to assess the error incurred by using jellium states in evaluating the matrix elements of the surface potential. Judging from the good agreement between theory and experiment it would seem that the approximation is well justified in the case of Cu but further work is needed to clarify the situation for other metals.

A second question concerns the Drude contribution introduced in Eqs. (42) and (43). This term accounts for the energy absorption mediated by phonon scattering in the bulk. In fitting to the experimental results for Cu, we obtained a room-temperature mean free path l of about 200 Å. This should be compared with $l\approx 400$ Å as obtained from dc conductivity measurements and with $l\approx 125$ Å as obtained from ir light reflection measurements. Now, the Drude formula is strictly valid only if the screened external electric field varies slowly in space on the length scale l. But in EELS the spatial variation of the electric field is determined by $q_{||}\sim k_0(\hbar\omega/2E_0)$, i.e., 10^{-2} Å^{-1} in our case. Thus, the electric field varies strongly over the length l and we are formally in the anomalous skin effect region. It is therefore not clear to what extent the phonon contribution can be represented by Eq. (43) and what the physical interpretation of the mean-free-path parameter l really is. These questions can only be settled by explicitly including electron-phonon interactions in the evaluation of the electron-hole pair production rate in Eq. (17). These considerations, of course, do not affect our conclusions regarding the zero-temperature pair production mechanism.

Finally, we note that there are several other interesting applications of the formalism presented in this work. For example, the surface response function $g(q_{||},\omega)$ determines (a) *the lifetime of excited states at surfaces;*[1,14] (b) *the van der Waals interaction between an atom and a surface;*[1,15] (c) *the surface power absorption;*[1] (d) *the friction force on a charged particle moving above metal surface;*[1,16] (e) *the surface photoelectric current.*[1,7] We refer the reader to the quoted references for details concerning these applications.

APPENDIX A

Here, we will prove (4). The electric potential outside the metal ($z>0$) is given by

$$\phi=(e^{q_{||}z}-ge^{-q_{||}z})e^{i(q_{||}\cdot x_{||}-\omega t)}+\text{c.c.}\equiv\phi_1+\phi_1^* . \quad \text{(A1)}$$

The power absorption is obtained by integrating the Poynting vector over the metal surface

$$\hbar\omega w = -\int d^2x \, \frac{c}{4\pi}\hat{\mathbf{z}}\cdot\mathbf{E}\times\mathbf{B} \, .$$

Now,

$$\mathbf{E} \approx -\nabla\phi \, ,$$

so that

$$\hbar\omega w = -\int d^2x \, \frac{c}{4\pi}\hat{\mathbf{z}}\cdot(-\nabla\phi)\times\mathbf{B}$$

$$= \frac{c}{4\pi}\int d^2x(\hat{\mathbf{z}}\times\nabla\phi)\cdot\mathbf{B}$$

$$= -\frac{c}{4\pi}\int d^2x \, \phi\hat{\mathbf{z}}\times\nabla\cdot\mathbf{B} = -\frac{c}{4\pi}\int d^2x \, \phi\hat{\mathbf{z}}\cdot\nabla\times\mathbf{B} \, .$$

But

$$\nabla\times\mathbf{B} = \frac{1}{c}\frac{\partial\mathbf{E}}{\partial t} \approx -\frac{1}{c}\frac{\partial}{\partial t}\nabla\phi \, ,$$

so that

$$\hbar\omega w = \frac{1}{4\pi}\int d^2x \, \phi\hat{\mathbf{z}}\cdot\frac{\partial}{\partial t}\nabla\phi = \frac{1}{4\pi}\int d^2x \, \phi\frac{\partial}{\partial t}\frac{\partial}{\partial z}\phi \, .$$

The time-averaged power absorption is thus

$$\hbar\omega w = \frac{1}{4\pi}\int d^2x \left\langle \phi\frac{\partial}{\partial t}\frac{\partial}{\partial z}\phi\right\rangle_{\text{av}}$$

$$= \frac{1}{4\pi}\int d^2x \left[\phi_1^*\frac{\partial}{\partial t}\frac{\partial}{\partial z}\phi_1 + \phi_1\frac{\partial}{\partial t}\frac{\partial}{\partial z}\phi_1^*\right]$$

$$= \frac{1}{2\pi}\text{Re}\left[\int d^2x \, \phi_1^*\frac{\partial}{\partial t}\frac{\partial}{\partial z}\phi_1\right] \tag{A2}$$

(where $\langle \ \rangle_{\text{av}}$ indicates time average). Substituting ϕ_1 from (A1) into (A2) gives

$$\hbar\omega w = \frac{1}{2\pi}\text{Re}\left[\int d^2x(1-g^*)(-i\omega q_{||})(1+g)\right]$$

$$= \frac{\omega q_{||}}{\pi}A \, \text{Im}g \, ,$$

so that

$$\text{Im}g = \frac{\pi\hbar w}{q_{||}A} \, ,$$

as given in (4).

APPENDIX B

In this appendix we shall derive some of the results of Sec. III from a slightly different point of view. We define the response function

$$f(q_{||},\omega) = \int dz \int dz' \, e^{q_{||}z}e^{q_{||}z'}\chi(z,z',q_{||},\omega) \tag{B1}$$

which is related to $g(q_{||},\omega)$ by

$$g(q_{||},\omega) = \frac{2\pi}{q_{||}}f(q_{||},\omega) \, . \tag{B2}$$

In the RPA, $f(q_{||},\omega)$ is given by

$$f(q_{||},\omega) = \int dz \int dz' \, \phi_{\text{ext}}(z)\chi^0(z,z',q_{||},\omega)\phi(z') \, , \tag{B3}$$

where ϕ_{ext} and ϕ are the potentials considered previously and χ^0 is the independent particle response function of the system. In particular (B3) gives

$$\text{Im}f(q_{||},\omega) = \int dz \int dz' \, \phi^*(z)\text{Im}\chi^0(z,z',q_{||},\omega)\phi(z') \, . \tag{B4}$$

For the jellium model we have

$$\text{Im}\chi^0(z,z',q_{||},\omega) = \frac{2}{\pi^3}\int d^2\mathbf{k}_{||}\int_0^\infty dk_z \int_0^\infty dk_z' \, f_{\mathbf{k}}(1-f_{\mathbf{k}'})u_{k_z}(z)u_{k_z'}(z)u_{k_z}(z')u_{k_z'}(z')\delta(\varepsilon_{\mathbf{k}'}-\varepsilon_{\mathbf{k}}-\omega) \, , \tag{B5}$$

where the wave vectors are

$$\mathbf{k} = \mathbf{k}_{||} + k_z\hat{z} \, ,$$

$$\mathbf{k}' = \mathbf{k}_{||} + \mathbf{q}_{||} + k_z'\hat{z} \, , \tag{B6}$$

and the wave functions $u_{k_z}(z)$ are solutions of the one-dimensional Schrödinger equation

$$-\frac{1}{2}\frac{d^2u_{k_z}(z)}{dz^2} + v(z)u_{k_z}(z) = \tfrac{1}{2}k_z^2u_{k_z}(z) \, . \tag{B7}$$

$v(z)$ is the potential confining the electrons in the metal. Substitution of (B5) into (B4) leads to a result consistent with (17). Here, we shall consider, however, the evaluation of $f(q_{||},\omega)$ only in the large η limit. It is then appropriate to use the $q_{||}\to 0$ limit of (B5) which for small ω is

$$\text{Im}\chi^0(z,z',0,\omega) = \simeq\omega\left[\frac{2}{\pi}\right]^2\int_0^{k_F}dk_z\int_{k_z}^{k_F}dk_z' \, u_{k_z}(z)u_{k_z}(z')u_{k_z'}(z)u_{k_z'}(z')\delta(\varepsilon_{k_z'}-\varepsilon_{k_z}-\omega) \, . \tag{B8}$$

We require the matrix elements

$$\langle k_z' \mid \phi_{\text{surf}} \mid k_z\rangle = -\frac{q_{||}}{2\pi}\int dz \, u_{k_z'}(z)A(z)u_{k_z}(z) \tag{B9}$$

and

$$\langle k_z' \mid \phi_{\text{bulk}} \mid k_z\rangle = -\frac{m_{\text{opt}}}{m}\left[\frac{2\omega^2}{\omega_p^2}\right]\int dz \, u_{k_z'}(z)u_{k_z}(z)e^{q_{||}z} \, . \tag{B10}$$

In particular, it can be shown that to order $q_{||}$.

$$\int dz\, e^{q_{||}z} u_{k_z'}(z) u_{k_z}(z) = \frac{q_{||}}{(\varepsilon_{k_z'} - \varepsilon_{k_z})^2} \int dz\, u_{k_z'}(z) \frac{dv}{dz} u_{k_z}(z) + O(q_{||}^2) \,. \tag{B11}$$

Using (B9)—(B11) together with (B8) in (B4), we find

$$\mathrm{Im} f(q_{||},\omega) = \omega q_{||}^2 \frac{1}{\pi^4} \int_0^{k_F} dk_z \frac{1}{k_z} \left| \left\langle k_z \left| \left[A - \frac{4\pi}{\omega_p^2} \frac{m_{\mathrm{opt}}}{m} \frac{dv}{dz} \right] \right| k_z \right\rangle \right|^2 . \tag{B12}$$

Finally we note that

$$\left\langle k_z \left| \frac{dv}{dz} \right| k_z \right\rangle = \tfrac{1}{2} k_z^2 \,, \tag{B13}$$

which follows on integrating by parts and making use of the Schrödinger equation (B7). Thus, from (B2) and (38) we obtain

$$\mathrm{Im} d_\perp(\omega) = \omega \frac{1}{\pi^3} \int_0^{k_F} dk_z \frac{1}{k_z} \left| \langle k_z \mid A \mid k_z \rangle - \frac{2\pi}{\omega_p^2} \frac{m_{\mathrm{opt}}}{m} k_z^2 \right|^2 . \tag{B14}$$

The coefficient of ω in (B14) gives $\bar{\xi}$ in (40) with

$$\xi = \frac{\omega_p k_F}{\pi^3} \int_0^{k_F} dk_z \frac{1}{k_z} \mid \langle k_z \mid A \mid k_z \rangle \mid^2 . \tag{B15}$$

Results for arbitrary η can be obtained using (B5), however in this case, the matrix element (B11) must be replaced by $\frac{1}{2} q_{||} / [q_{||}^2 + (k_z - k_z')^2]$. One then finds the results quoted in Sec. III.

---

*Permanent address: Department of Physics, Queen's University, Kingston, Canada K7L 3N6.

[1]See, e.g., P. J. Feibelman, Prog. Surf. Sci. **12**, 287 (1982).

[2]K. L. Kliewer, Surf. Sci. **101**, 57 (1980); G. Mukhopadhyay and S. Lundqvist, Phys. Scr. **17**, 69 (1978); F. Forstmann and R. R. Gerhards, in *Festkörperprobleme, Advances in Solid State Physics,* edited by J. Treusch (Vieweg, Brauschweigh, 1982), Vol. 22, p. 291.

[3]P. J. Feibelman, Phys. Rev. B **22**, 3654 (1980); **12**, 1319 (1975); **14**, 762 (1976); **9**, 5077 (1974).

[4]B. N. J. Persson and N. D. Lang, Phys. Rev. B **26**, 5409 (1982); B. N. J. Persson and S. Andersson, *ibid.* **29**, 4382 (1984).

[5]A. G. Eguiluz, Phys. Rev. Lett. **51**, 1907 (1983).

[6]N. D. Lang and W. Kohn, Phys. Rev. B **1**, 4555 (1970).

[7]H. J. Levinson, E. W. Plummer, and P. J. Feibelman, Phys. Rev. Lett. **43**, 952 (1979).

[8]B. N. J. Persson and P. Apell, Phys. Rev. B **27**, 6058 (1983).

[9]The expression for $\eta(r_s)$ given in Ref. 8 is in error which is corrected in B. N. J. Persson and E. Zaremba, Phys. Rev. B **30**, 5669 (1984).

[10]S. Andersson and B. N. J. Persson, Phys. Rev. Lett. **50**, 2028 (1983).

[11]See, e.g., A. A. Lucas and M. Sunjic, Phys. Rev. Lett. **26**, 229 (1971); H. Ibach and D. L. Mills, *Electron Energy Loss Spectroscopy and Surface Vibrations* (Academic, New York, 1982); B. N. J. Persson, Surf. Sci. **92**, 265 (1980).

[12]See, the work by Persson in Ref. 11.

[13]S. Andersson, B. N. J. Persson, M. Persson, and N. D. Lang, Phys. Rev. Lett. **50**, 2028 (1983).

[14]H. Morawitz, Phys. Rev. **187**, 1792 (1969); R. R. Chance, A. Prock, and R. Silbey, Adv. Chem. Phys. **37**, 1 (1978); B. N. J. Persson and M. Persson, Surf. Sci. **3**, 609 (1980).

[15]E. Zaremba and W. Kohn, Phys. Rev. B **13**, 2270 (1976); B. N. J. Persson and P. Apell, *ibid.* **27**, 6058 (1983); B. N. J. Persson and E. Zaremba, *ibid.* **30**, 5669 (1984).

[16]E. G. D'Agliano, P. Kumar, W. L. Schaich, and H. Suhl, Phys. Rev. B **11**, 2122 (1975).

[17]N. D. Lang and W. Kohn, Phys. Rev. B **7**, 3541 (1973).